Nonlocal Means-Based Speckle Filtering for Ultrasound Images

Ammar Amin

***Abstract*-Aiming at the problem of unclear images acquired in interactive systems, an image processing algorithm for nonlocal mean denoising is proposed. The experimental results show that compared with the traditional method of adaptive filtering like Lee's filter, Frost's filter, Kuan's filter, etc the algorithm proposed in this paper has better results in the visual quality and peak signal-to-noise ratio (PSNR) of complex noise images. Results on real images demonstrate that the proposed method can able to preserve accurately edges and structural details of image.**

***Index Terms*—Speckle, Nl-means, Multiscale, Adaptive Filters, PSNR, Variance, Image Size, Computational Time, 2D ultrasound.**

I. INTRODUCTION

The goal of image denoising methods is to recover the original image from a noisy measurement. Several methods have been proposed to remove the noise and recover the true image u. Even though they may be very different in tools it must be emphasized that a wide class share the same basic remark: denoising is achieved by averaging. This averaging may be performed locally: the Gaussian smoothing model or non-locally: non-local means smoothing model. Here in this paper, we kept the emphasis on the non-local means smoothing model [1] inspired by Buades et al. We propose and analyze the NL-means algorithm, which is defined by the simple formula

$$NL[v](i) = \sum_{j \in I} w(i,j)v(j),$$

Given a discrete noisy image v = {v(i) | i ∈ I}, the estimated value NL[v](i), for pixel i, is computed as a weighted average of all the pixels in the image, where the family of weights {w(i, j)}j depends on the similarity between the pixels i and j. For a more detailed analysis of the NL-means algorithm and a more complete comparison, see further section II where we discussed an overview of speckle filters and related methods. Section III described the proposed Bayesian NL-means filter adapted to speckle noise. Quantitative results on artificial images with various noise models are presented in Section IV. Finally, qualitative results on real 2-D and 3-D US images are proposed in Section V.

II. SPECKLE REDUCTION- RELATED WORK

Speckle is a granular interference that inherently exists in and degrades the quality of medical ultrasounds. Scattered signals add coherently; that is, they add constructively and destructively. Below is an example of a noise model generated in MATLAB for different variance and zero mean. of speckle noise.

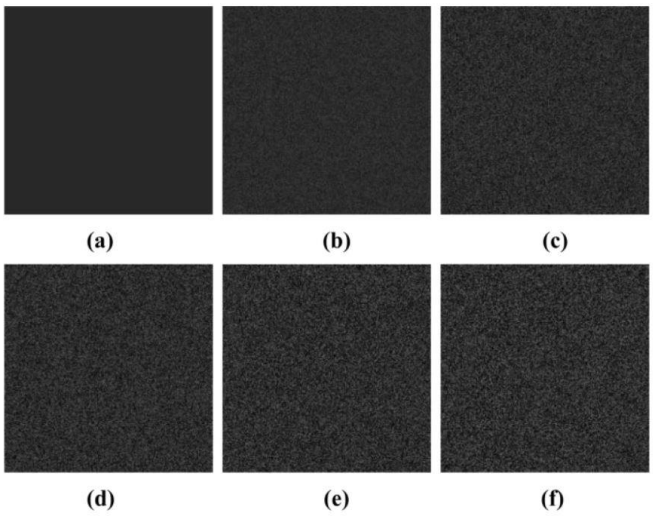

Fig 1. Experimental images generated by MATLAB: (a) original image; (b) Var = 0.1; (c) Var = 0.3; (d) Var = 0.5; (e) Var = 0.7; (f) Var= 0.9

A. Adaptive Filters

The adaptive filters are widely used in US image restoration because they are easy to implement and control. The commonly used adaptive filters—the Lee's filter [5], Frost's filter [6], and Kuan's filter [7]—assume that speckle noise is essentially a multiplicative noise.

Lee's Filter is based on the approach that smoothing is performed on low variance areas. However, smoothing will not be performed on the area of high variance, which is near edges however The Kuan's filter is a generalization of Lee's filter. Kuan's filter converts the multiplicative model of

speckle into an additive linear form. Unlike the Lee filter, smoothing is also performed near edges.

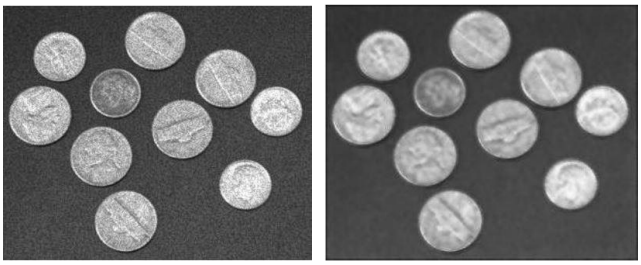

Fig 2. Lee's filter denoising of the speckle noise on a coin dataset.

B. Multiscale Methods

The wavelet transform performs the multi-scale analysis of the given image by treating low and high-frequency components present in an image separately. The wavelet transform decomposes the given image into detail and approximation sub-band. It is assumed that the approximation sub-band contains significant structures and the detail sub-band may contain noise. So, the filtering process is more for noise content, and less in the presence of significant image structures. The filtering process performs non-linear thresholding of wavelet coefficients. The first task is to find threshold value and the second task is to use the thresholding rule over wavelet coefficients for the calculated threshold value. The researchers have developed many different techniques for finding threshold value as mentioned in [23]–[25] and various methods for speckle reduction have also been investigated in [26]-[28].

C. Hybrid Approaches

The above-mentioned approaches can be also combined in order to take advantage of the different paradigms. In [38], the image is preprocessed by an adaptive filter in order to decompose the image into two components. A Donoho's soft thresholding method is then performed on each component. Finally, the two processed components are combined to reduce speckle. PDE-based approaches and a wavelet transform have been also combined as proposed in [39].

III. METHOD

The previously mentioned approaches for speckle reduction are based on the so-called locally adaptive recovery paradigm [40]. Nevertheless, more recently, a new patch-based nonlocal recovery paradigm has been proposed by Buades et al. [1]. This new paradigm proposes to replace the local comparison of pixels with the nonlocal comparison of patches. In this section, we rather revise the traditional formulation of the NL-means filter, suited to the additive white Gaussian noise model, and adapt this filter to spatial speckle patterns.

A. Nonlocal Means Filter

Given a discrete noisy image v = {v(i) | i ∈ I}, the estimated value NL[v](i), for a pixel i, is computed as a weighted average of all the pixels in the image

$$NL[v](i) = \sum_{j \in I} w(i,j)v(j),$$

where the family of weights {w(i, j)}j depends on the similarity between the pixels i and j.

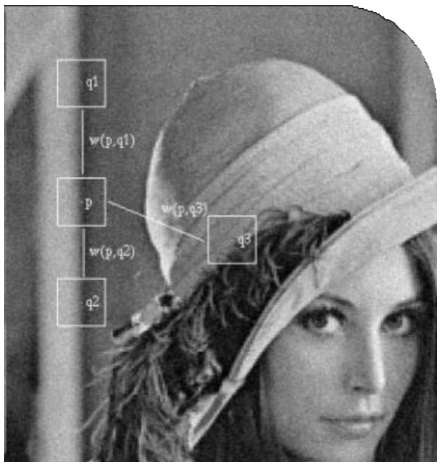

Fig 3. w(p,q1) and w(p,q2) have a larger weight while many different neighborhoods give a small weight w(p,q3).

The similarity between two pixels i and j depends on the similarity of the intensity gray level vectors v(Ni) and v(Nj), where Nk denotes a square neighborhood of fixed size and centered at a pixel k. This similarity is measured as a decreasing function of the weighted Euclidean distance. The application of the Euclidean distance to the noisy neighborhoods raises the following equality.

$$E||v(\mathcal{N}_i) - v(\mathcal{N}_j)||^2_{2,a} = ||u(\mathcal{N}_i) - u(\mathcal{N}_j)||^2_{2,a} + 2\sigma^2.$$

This equality shows the robustness of the algorithm since in expectation the Euclidean distance conserves the order of similarity between pixels. The pixels with a similar grey level neighborhood to v(Ni) have larger weights in the average, see Figure 3. These weights are defined as

$$w(i,j) = \frac{1}{Z(i)} e^{-\frac{||v(\mathcal{N}_i) - v(\mathcal{N}_j)||^2_{2,a}}{h^2}},$$

Here Z(i) acts as a Normalizing constant and the parameter h acts as a degree of filtering. It controls the decay of the exponential function and therefore the decay of the weights as a function of the Euclidean distances. The NL-means not only compares the grey level in a single point but the geometrical configuration in a whole neighborhood. This fact allows a more robust comparison than neighborhood filters. Figure 3 illustrates this fact, the pixel q3 has the same grey level value of pixel p, but the neighborhoods are much different, and therefore the weight w(p, q3) is nearly zero.

IV. SYNTHETIC IMAGE EXPERIMENTS

In this section, we propose to compare different filters with experiments on synthetic data, with different noise models.

1. In Section IV-A, a base image lena.jpg is selected and a noise model available in MATLAB is considered for the experiments, and the Peak signal-to-noise ratio (PSNR) is used to compare objectively the effect of the nl-means filter on various images.

2. In Section IV-B, we proposed various image quality assessment parameters, their effect, and outcomes on various noise models and we calculate the computational burden on the CPU for various image sizes and their relationship.

A. 2D image lena.jpg corrupted by Theoretical (MATLAB) noise model

In this experiment, the synthetic image "Lena.jpg" (see Fig. 4), was corrupted with different levels of noise. The image is a greyscale image of 347×497 pixels, with a square search volume of 11×11.

Variance= 0.1, h=30

Variance= 0.2, h=40

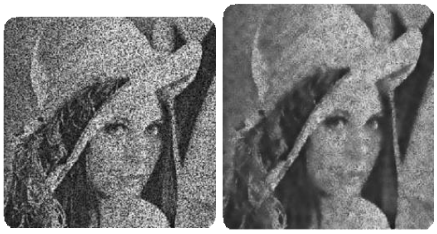

Variance= 0.5, h=50

Fig 4. Speckle noise addition of different variance to base image and filtering using nl means

Filter	Variance	Smoothing parameter(h)	Patch size
NL-means filter	0.1	30	5×5
	0.2	40	
	0.4	50	

The above table shows various parameters of filtering using nl-means on lena.jpg. Three levels of noise were tested by setting variance={0.1, 0.2, 0.5}. To assess denoising methods, the PSNR values were computed between the "ground truth" and the denoised images.

$$PSNR = 10\log_{10}(peakval^2/MSE)$$

peakval is either specified by the user or taken from the range of the image data type (here used 255

Peak SNR(dB)			
Filter	∂=0.1	∂=0.2	∂=0.4
Noisy Image	16.1572	13.39	10.85
Nl-means	22.9	20.46	17.41

B. Image quality assessment parameters and Computational Burden.

Image quality is important when evaluating or segmenting ultrasound images, where speckle obscures subtle details in the image. The statistical parameters like Signal to Noise Ratio(SNR), Correlation Coefficient(CC), variance, MSE, and Peak Signal to Noise Ratio (PSNR) are used for image quality assessment. Here, we will discuss PSNR as a metric for image quality assessment.

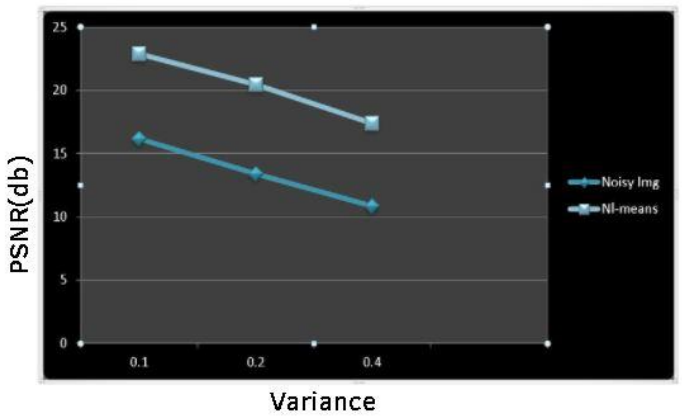

Above is the graph of PSNR vs Variance of Lena.jpg for both noise-induced image and nl-means filtered image. We can see that the PSNR value for Nl-means for each variance

is higher than the noisy image which shows that Nl-means provide a more filtered image compared to the ground truth of the noisy image. Thus Nl-means is capable of removing speckle noise from the image.

Computational Burden: The computational time of a filter is the time taken by a digital computing platform to execute the filtering algorithm when no other software, except the operating system, runs on it. It depends on the computing system's clock time period. But, in addition to the clock period, it depends on the memory size, the input data size, and the memory access time, etc.

System Requirement	Image Size(Pixels)	Computational time(sec)
Device name LAPTOP-MRAUD0QK Processor Intel(R) Core(TM) i5-8250U CPU @ 1.60GHz 1.80 GHz Installed RAM 8.00 GB Nvidia- GPU 4.00GB	200×200	10.38 sec
	374×497	40.8 sec
	617×617	79.0 sec

The above table shows the computational time taken by the algorithm on the mentioned device for different test image sizes.

V. EXPERIMENTS ON REAL DATA

In this section, a visual comparison of 2-D ultrasound images of liver hepatic vein, heart, and gall bladder has been worked on to remove speckle noise from the dataset.

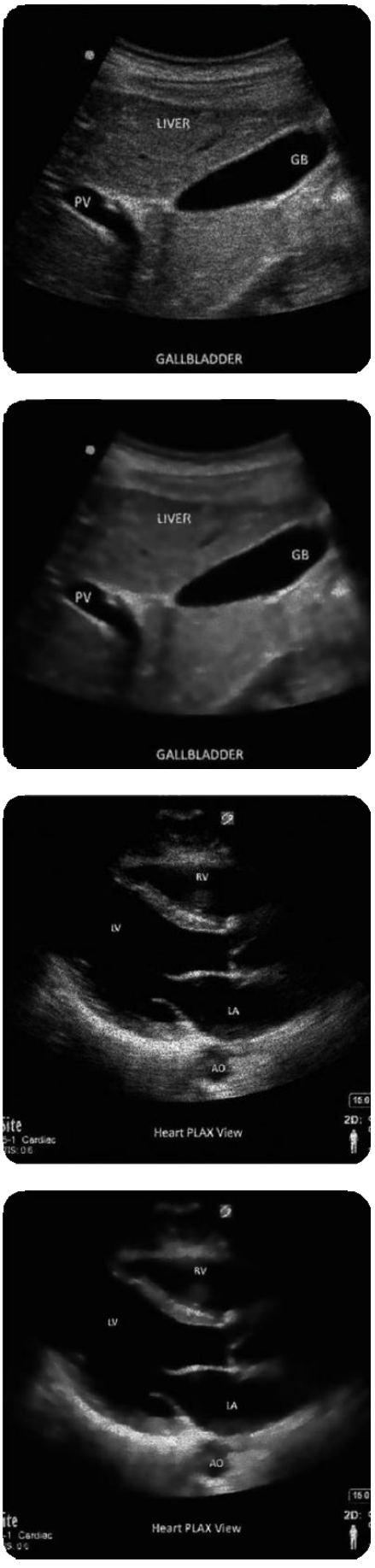

Fig 5. Results obtained after speckle filtering using Nl-means for 2-D ultrasound images of liver hepatic vein, heart, and gall bladder respectively

VI. CONCLUSION AND FUTURE WORK

In this paper, a despeckling method, based on Nl-means has been proposed. Experiments were carried out on synthetic images with different simulations of speckle. During the experiments, quantitative measures were used to compare several denoising parameters. The experimental results demonstrate its efficacy both in terms of speckle reduction and computational time required for denoising.

For future work, Optimised Bayesian NL- means (OBNLM) can be implemented to improve the quality of the filtered image and the algorithm can be implemented on multi-dimensional images to enhance the efficacy and user experience.

REFERENCES

[1] A. Buades, B. Coll, and J. M. Morel, "A review of image denoising algorithms, with a new one," Multiscale Model. Simul., vol. 4, no. 2, pp. 490–530, 2005.

[2] S. P. Awate and R. T. Whitaker, "Unsupervised, information-theoretic, adaptive image filtering for image restoration," IEEE Trans. Pattern Anal. Mach. Intell., vol. 28, no. 3, pp. 364–376, Mar. 2006.

[3] C. Kervrann, J. Boulanger, and P. Coupé, "Bayesian non-local means filter, image redundancy and adaptive dictionaries for noise removal," in Proc. Conf. Scale-Space and Variational Methods, Ischia, Italy, Jun. 2007, pp. 520–532.

[4] T. Loupas, W. McDicken, and P. Allan, "An adaptive weighted median filter for speckle suppression in medical ultrasound image," IEEE Trans. Circuits Syst., vol. 36, pp. 129–135, 1989.

[5] J. S. Lee, "Digital image enhancement and noise filtering by use of local statistics," IEEE Trans. Pattern Anal. Mach. Intell., vol. PAMI-2, pp. 165–168, 1980.

[6] V. Frost, J. Stiles, K. Shanmugan, and J. Holtzman, "A model for radar images and its application to adaptive digital filtering of multiplicative noise," IEEE Trans. Pattern Anal. Mach. Intell., vol. PAMI-2, pp. 157–65, 1982.

[7] D. Kuan, A. Sawchuck, T. Strand, and P. Chavel, "Adaptive noise smoothing filter for images with signal-dependent noise," IEEE Trans. Pattern Anal. Mach. Intell., vol. PAMI-7, no. 2, pp. 165–177, Feb. 1985.

[8] A. Lopes, R. Touzi, and E. Nezry, "Adaptive speckle filters and scene heterogeneity," IEEE Trans. Geosci. Remote Sens., vol. 28, pp. 992–1000, 1990.

[9] M. Karaman, M. A. Kutay, and G. Bozdagi, "An adaptive speckle suppression filter for medical ultrasonic imaging," IEEE Trans. Med. Imag., vol. 14, pp. 283–292, 1995.

[10] E. Kofidis, S. Theodoridis, C. Kotropoulos, and I. Pitas, "Nonlinear adaptive filters for speckle suppression in ultrasonic images," Signal Process., vol. 52, no. 3, pp. 357–72, 1996.

[11] J. M. Park, W. J. Song, and W. A. Pearlman, "Speckle filtering of sar images based on adaptive windowing," Vis., Image, Signal Process., vol. 146, no. 4, pp. 191–197, 1999.

[12] P. C. Tay, S. T. Acton, and J. A. Hossack, "A stochastic approach to ultrasound despeckling," in Proc. 3rd IEEE Int. Symp. Biomedical Imaging: Nano to Macro, 2006, pp. 221–224.

[13] P. C. Tay, S. T. Acton, and J. A. Hossack, "Ultrasound despeckling using an adaptive window stochastic approach," in Proc. IEEE Int. Conf. Image Processing, 2006, pp. 2549–2552.

[14] T. C. Aysal and K. E. Barner, "Rayleigh-maximum-likelihood filtering for speckle reduction of ultrasound images," IEEE Trans. Med. Imag., vol. 26, pp. 712–727, 2007.

[15] P. Perona and J. Malik, "Scale-space and edge detection using anisotropic diffusion," IEEE Trans. Pattern Anal. Mach. Intell., vol. 12, no. 7, pp. 629–639, Jul. 1990.

[16] L. Rudin, S. Osher, and E. Fatemi, "Nonlinear total variation based noise removal algorithms," Phys. D, vol. 60, pp. 259–268, 1992.

[17] Y. Yu and S. T. Acton, "Speckle reducing anisotropic diffusion," IEEE Trans. Image Process., vol. 11, pp. 1260–1270, 2002.

[18] Y. Yu, J. A. Molloy, and S. T. Acton, "Three-dimensional speckle reducing anisotropic diffusion," in , Proc. 37th Asilomar Conf. Signals, Systems and Computers, 2003, vol. 2, pp. 1987–1991.

[19] K. Z. Abd-Elmoniem, A. B. Youssef, and Y. M. Kadah, "Real-time speckle reduction and coherence enhancement in ultrasound imaging via nonlinear anisotropic diffusion," IEEE Trans. Biomed. Eng., vol. 49, pp. 997–1014, 2002.

[20] K. Krissian, C. F. Westin, R. Kikinis, and K. G. Vosburgh, "Oriented speckle reducing anisotropic diffusion," IEEE Trans. Image Process., vol. 16, pp. 1412–1424, 2007.

[21] C. Sheng, Y. Xin, Y. Liping, and S. Kun, "Total variation-based speckle reduction using multi-grid algorithm for ultrasound images," in Proc. Int. Conf. Image Analysis and Processing, 2005, vol. 3617, pp. 245–252.

[22] K. Djemal, "Speckle reduction in ultrasound images by minimazation of total variation," in Proc. Int. Conf. Image Processing, 2005, vol. 3, pp. 357–360.

[23] D. Donoho and I. Johnstone, "Ideal spatial adaptation by wavelet shrinkage," Biometrika, vol. 81, no. 3, pp. 425–455, 1994.

[24] D. Donoho, "De-noising by soft-thresholding," IEEE Trans. Inf. Theory, vol. 41, pp. 613–627, 1995.

[25] R. Coifman and D. Donoho, "Translation invariant de-noising," in Lecture Notes in Statistics: Wavelets and Statistics. New York: LCNS, 1995, pp. 125–150.

[26] J. E. Odegard, H. Guo, M. Lang, C. S. Burrus, R. O. Wells, L. M. Novak, and M. Hiett, "Wavelet based SAR speckle reduction and image compression," in Proc. SPIE Algorithms for Synthetic Aperture, 1995, vol. 2487, pp. 259–271.

[27] L. Gagnon and D. F. Smaili, O. E. Drummond, Ed., "Speckle noise reduction of airborne sar images with symmetric daubechies wavelets," in Proc. SPIE Signal and Data Processing of Small Targets, 1996, vol. 2759, pp. 14–24.

[28] X. Zong, A. F. Laine, and E. A. Geiser, "Speckle reduction and contrast enhancement of echocardiograms via multiscale nonlinear processing," IEEE Trans. Med. Imag., vol. 17, pp. 532–540, 1998.

[29] A. Pizurica, A. M. Wink, E. Vansteenkiste, W. Philips, and J. Roerdink, "A review of wavelet denoising in mri and ultrasound brain imaging," Curr. Med. Imag. Rev., vol. 2, no. 2, pp. 247–260, 2006.

[30] A. Achim, A. Bezerianos, and P. Tsakalides, "Novel Bayesian multiscale method for speckle removal in medical ultrasound images," IEEE Trans. Med. Imag., vol. 20, pp. 772–783, Aug. 2001.

[31] S. Foucher, G. B. Benie, and J. M. Boucher, "Multiscale map filtering of sar images," IEEE Trans. Image Process., vol. 10, pp. 49–60, 2001.

[32] S. Gupta, R. C. Chauhan, and S. C. Saxena, "Locally adaptive wavelet domain Bayesian processor for denoising medical ultrasound images using

speckle modelling based on rayleigh distribution," Proc. IEEE Vision, Image and Signal Processing, vol. 152, no. 1, pp. 129–135, 2005.

[33] M. I. H. Bhuiyan, Omair, and M. N. S. Swamy, "New spatially adaptive wavelet-based method for the despeckling of medical ultrasound images," in Proc. IEEE Int. Symp. Circuits and Systems, 2007, pp. 2347–2350.

[34] Z. Yang and M. D. Fox, "Speckle reduction and structure enhancement by multichannel median boosted anisotropic diffusion," EURASIP J. Appl. Signal Process., vol. 2004, no. 1, pp. 2492–2502, Jan. 2004.

[35] O. Acosta, H. Frimmel, A. Fenster, and S. Ourselin, "Filtering and restoration of structures in 3d ultrasound images," in Proc. IEEE 4th Int. Symp. Biomedical Imaging: From Nano to Macro, 2007, pp. 888–891.

[36] F. Zhang, Y. M. Yoo, L. M. Koh, and Y. Kim, "Nonlinear diffusion in Laplacian pyramid domain for ultrasonic speckle reduction," IEEE Trans. Med. Imag., vol. 26, pp. 200–211, 2007.

[37] B. Aiazzi, L. Alparone, and S. Baronti, "Multiresolution local-statistics speckle filtering based on a ratio Laplacian pyramid," IEEE Trans. Geosci. Remote Sens., vol. 36, pp. 1466–1476, 1998.

[38] X. Hao, S. Gao, and X. Gao, "A novel multiscale nonlinear thresholding method for ultrasonic speckle suppressing," IEEE Trans. Med. Imag., vol. 18, pp. 787–794, 1999.

[39] A. Ogier, P. Hellier, and C. Barillot, "Restoration of 3D medical images with total variation scheme on wavelet domains (TVW)," in Proc. SPIE Med. Imag., Feb. 2006, vol. 6144.

[40] M. Elad, "On the origin of the bilateral filter and ways to improve it," IEEE Trans. Image Process., vol. 11, pp. 1141–1151, 2002.

[41] C. Kervrann and J. Boulanger, "Optimal spatial adaptation for patchbased image denoising," IEEE Trans. Image Process., vol. 15, 2006.

[42] S. Kindermann, S. Osher, and P. W. Jones, "Deblurring and denoising of images by nonlocal functionals," Multiscale Model. Simul., vol. 4, no. 4, pp. 1091–1115, 2005.

[43] H. Q. Luong, A. Ledda, and W. Philips, "Non-local image interpolation," in Proc. IEEE Int. Conf. Image Processing, 2006, pp. 693–696.

[44] T. Brox and D. Cremers, "Iterated nonlocal means for texture restoration," presented at the Int. Conf. Scale Space and Variational Methods in Computer Vision, Ischia, Italy, May 2007.

[45] C. Kervrann and J. Boulanger, "Local adaptivity to variable smoothness for exemplar-based image regularization and representation," Int. J. Comput. Vis., to be published.

[46] P. Coupé, P. Yger, S. Prima, P. Hellier, C. Kervrann, and C. Barillot, "An optimized blockwise non local means denoising filter for 3D magnetic resonance images," IEEE Trans. Med. Imag., vol. 27, pp. 425–441, 2008.

[47] Z. Tao, H. D. Tagare, and J. D. Beaty, "Evaluation of four probability distribution models for speckle in clinical cardiac ultrasound images," IEEE Trans. Med. Imag., vol. 25, pp. 1483–1491, 2006.

[48] G. Slabaugh, G. Unal, T. Fang, and M. Wels, "Ultrasound-specific segmentation via decorrelation and statistical region-based active contours," in Proc. IEEE Computer Society Conf. Computer Vision and Pattern Recognition, 2006, vol. 1, pp. 45–53.

[49] K. Krissian, K. Vosburgh, R. Kikinis, and C.-F. Westin, "Speckle-constrained anisotropic diffusion for ultrasound images," presented at the IEEE Computer Society Conf. Computer Vision and Pattern Recognition, Jun. 2005.

[50] F. Argenti and G. Torricelli, "Speckle suppression in ultrasonic images based on undecimated wavelets," EURASIP J. Adv. Signal Process., vol. 2003, no. 5, pp. 470–478, 2003.

[51] M. P. Wachowiak, A. S. Elmaghraby, R. Smolíkova, and J. M. Zurada, "Classification and estimation of ultrasound speckle noise with neural networks," in Proc. IEEE Int. Symp. Bio-Informatics and Biomedical Engineering, 2000, pp. 245–252.

[52] D. Sakrison, "On the role of the observer and a distortion measure in image transmission," IEEE Trans. Commun., vol. 25, pp. 1251–1267, 1977.

[53] J. A. Jensen, "Field: A program for simulating ultrasound systems," Med. Biol. Eng. Comput., vol. 34, pp. 351–353, 1996.

[54] P. Coupé, P. Hellier, X. Morandi, and C. Barillot, "Probe trajectory interpolation for 3D reconstruction of freehand ultrasound," Med. Image Anal., vol. 11, no. 6, pp. 604–615, 2007.

[55] F. Godtliebsen, E. Spjotvoll, and J. S. Marron, "A nonlinear Gaussian filter applied to images with discontinuities," J. Nonparametr. Statist., vol. 8, no. 1, pp. 21–43, 1997.